



Neuroscience

Report on the module: Neuroprosthetics

Faculty VI

Uni Oldenburg – May 6th to May 23rd 2019

Date of submission: August 6th 2019

Summer term 2019

supervisors:

Mathias Dietz, Sven Hermann

Issued by: Yannik Karsten

student number: 3007397

Email: yannik.karsten@uni-oldenburg.de

Disclaimer

The following report builds on the topics covered in the lecture and exercise and thus the main script of Prof. Werner Hemmert and Jörg Encke "Neuroprothetics" serves as an intellectual basis. Derivations of formulas and theoretical background knowledge are taken from this script. Formulations have been changed and interpreted by me but should not be taken as plagiarism. If text passages are not marked as quotations, this is an omission and reference should be made to the source mentioned above.

Matlab and python code were written by me and the plots are from my own hand.

Introduction

Damage to the hair cells in the inner ear (cochlea) is referred to as sensori-neural hearing loss. Anyone suffering from such a hearing loss in Germany is usually entitled to a cochlear implant (CI). This is an electronic medical device that perceives the function of the damaged inner ear and thus enables hearing. A sound processor worn behind the ear captures acoustic signals and converts them into a digital signal using various algorithms. A battery or rechargeable battery module in the Sound Processor supplies power to the entire system. The Sound Processor transmits the digitally coded signal through the induction coil attached to the side of the head to the implant under the skin. The implant converts the digitally coded audio signal into electrical currents and transmits them to the electrode array in the cochlea. The implant electrodes primarily stimulate the spiral ganglia of the cochlea, whose afferent axons bundle to form the auditory nerve, from where the signal impulses are transmitted to the brain. This is where the auditory perception emerges.

In the Course, models were programmed that simulate how nerve cells behave during electrical stimulation. Based on this, various components were programmed to simulate the functionality of a CI as a whole. These models were used to identify physical and neurobiological hurdles that are crucial for the implementation of CI algorithms. In the following, the most important concepts are explained, followed by the respective computer models, which take these concepts into account.

Neuron

Nerve cells have a semipermeable membrane, which serves as both an insulator and a diffusion barrier to the movement of ions. Embedded in this membrane are so called transmembrane proteins (ion pumps), they actively move ions across the membrane, thus causing a concentration gradient. Passive movement of the ions along the gradient is made possible by ion-channels. Patch clamp experiments have shown that the current across a membrane fluctuates between zero and a distinct state. This phenomenon can be explained by the assumption that a single channel must be either fully open or closed at all times without an intermediate state. The proportional time that the channel is open can thus be understood as the opening probability of this ion channel. The current of an ion type across the membrane thus depends on the opening probability of the respective channel.

Ion-pumps and -channels are electrically equivalent to a set of batteries and resistors inserted in the membrane, and therefore create a voltage between the two sides of the membrane, the membrane potential (compare to Figure 1:Figure 1). In dormant neurons, without external inputs the membrane potential typically rests within -40 mV to -80 mV . In the advent of a stimulus the membrane potential may rise or fall due to specific changes in membrane permeabilities for potassium, sodium, calcium, and chloride ions. In case the potential exceeds the threshold value (typically 15 mV above resting potential), voltage gated ion channels open. This leads to an action potential (AP), caused by an influx

of sodium ions into the cell and a rapid change in membrane potential. Followed by a refractory period in which the resting potential is being restored and the cell is less likely to spike.

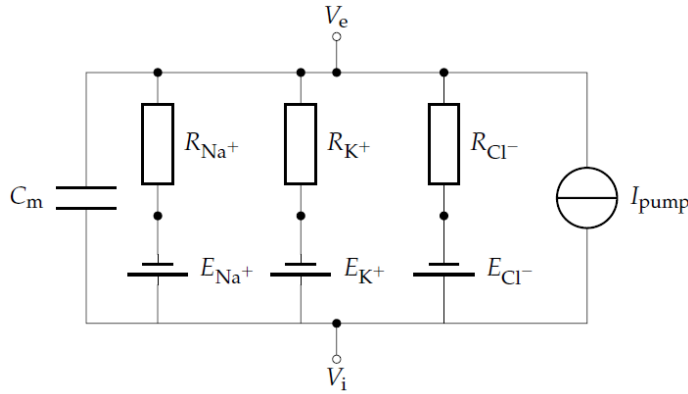


Figure 1: “A equivalent circuit of the cell at resting potential. Each ion species is represented as a resistor and a battery. The battery represents the ions Nernst potential while the resistor defines how permeable the membrane is for this type of ion. The membrane is implemented as a capacity and the ions pumps as a simple current source.” Hemmert, W.; Encke J. (2017) p.9

The equivalent circuit and Kirchhoff's first law

As described above, the neuron can also be displayed schematically as an equivalent circuit. In this case, the membrane is implemented as an electric capacity c_m and the different types of ions as a battery in series to a resistor (see Figure 1). The battery represents the Nernst potential of the single ion species. That is the electrical potential generated across the membrane at electrochemical equilibrium. It is generally expressed by this equation:

$$E_X = \frac{RT}{zF} \ln \frac{[X]_{out}}{[X]_{in}} \quad (1)$$

“Where E_X is the equilibrium potential for any ion X, R is the gas constant, T is the absolute temperature, z is valence (electrical charge) of the permeant ion and F is the Faraday constant (the amount of electrical charge contained in one mole of a univalent ion).” Purves et al. (2012, p. 33) The resistor in the circuit is dependent on the permeability for the particular type of ions.

In order to calculate the current across each individual cell, Kirchhoff's first law is needed: “In a node of an electrical network, the sum of the incoming currents is equal to the sum of the outgoing currents.”

$$\sum_{k=1}^n I_k = 0 \quad (2)$$

If the transmembrane voltage is described as:

$$V_m = V_i - V_e \quad (3)$$

the following equation is obtained:

$$0 = C_m \frac{dV_m}{dt} + I_{Na} + I_K + I_{Cl} + I_{pump} \quad (4)$$

$$C_m \frac{dV_m}{dt} = - \left(\frac{V_m - E_{Na}}{R_{Na}} + \frac{V_m - E_K}{R_K} + \frac{V_m - E_{Cl}}{R_{Cl}} + I_{pump} \right) \quad (5)$$

This equation shows that the influence of the Nernst potential is proportional to the membrane conductivity $g_x = 1/R_x$ for a given type of ion (X). The influence of the ion pump can be neglected relative to the net conductivity of the membrane in most cases.

Leaky integrate and fire neuron (LIF)

The first modelling approach was the most basic type of model, a mere passive description of the membrane, showing the characteristics mentioned above. For this application Figure 1 can be simplified, by replacing the batteries as well as the resistors with a combined leak conductance g_{leak} and a battery setting the resting potential E_{rest} (Figure 3). In this case, the ion pump can be dispensed with, as the resting potential is maintained by the battery.

Kirchhoff's law, as described above, can be applied to this simplified equivalent circuit as well:

$$0 = I_c + I_{leak} \quad (6)$$

$$0 = C_m \frac{dV_m}{dt} + g_{leak}(E_{rest} - V_m) \quad (7)$$

Further simplifications can be made, by introducing the time constant τ (tau) into the equation. In a decaying system, the time constant is the time for the system's step response to reach $1/e \approx 36.8\%$ of its final (asymptotic) value i.e. the resting potential.

$$\tau_m = c_m * R_{leak} \quad (8)$$

$$\frac{dV_m}{dt} = \frac{1}{\tau_m}(E_{rest} - V_m) \quad (9)$$

To stimulate the neuron, another current source I_{stim} is introduced in parallel to the capacity. This current source can be thought of as a patch electrode injecting a current into the neuron.

$$\frac{dV_m}{dt} = \frac{1}{c_m} I_{stim} dt + \frac{1}{\tau_m} (E_{rest} - V_m) dt \quad (10)$$

$$V_m = \int \frac{1}{c_m} I_{stim} dt + \int \frac{1}{\tau_m} (E_{rest} - V_m) dt \quad (11)$$

When considering the equation, it is noticeable that the first part integrates over the input current by charging the membrane capacity, while the second part tries to move the membrane potential back to resting potential by leaking some charge through g_{leak} . That is the reason why this model is called the leaky integrate and fire (LIF) model.

If a constant current is used, the analytical equation can be formulated as follows:

$$V_m = I_{stim} R_m (1 - e^{-t/\tau}) + V_{rest} \quad (12)$$

This highly simplified model is only able to map the charge of the membrane. The triggering of action potentials is added manually for the time being. For this purpose, a threshold value V_{thr} is defined; if this value is exceeded, the voltage is set to a maximum value V_{spike} and at the next point in time is shifted back to the rest potential V_{rest} . This results in the following calculation rules:

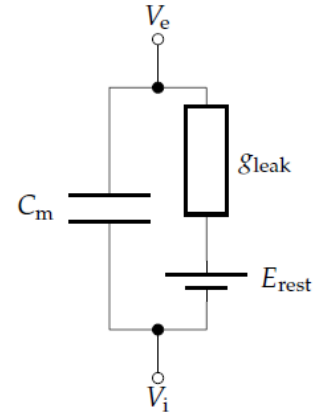


Figure 2: "Equivalent circuit of a simple, passive cellular membrane." Hemmert, W.; Encke J. (2017) p. 19

$$\frac{dV_m}{dt} = \frac{1}{C_m} I_{stim} + \frac{1}{\tau_m} (E_{rest} - V_m) \quad \text{if } V_m < V_{thr} \quad (13)$$

$$V_m = V_{spike} \quad \text{if } V_m = V_{thr} \quad (14)$$

$$V_m = V_{rest} \quad \text{if } V_m = V_{spike} \quad (15)$$

This model was implemented using Python v3.7 (Figure 4).

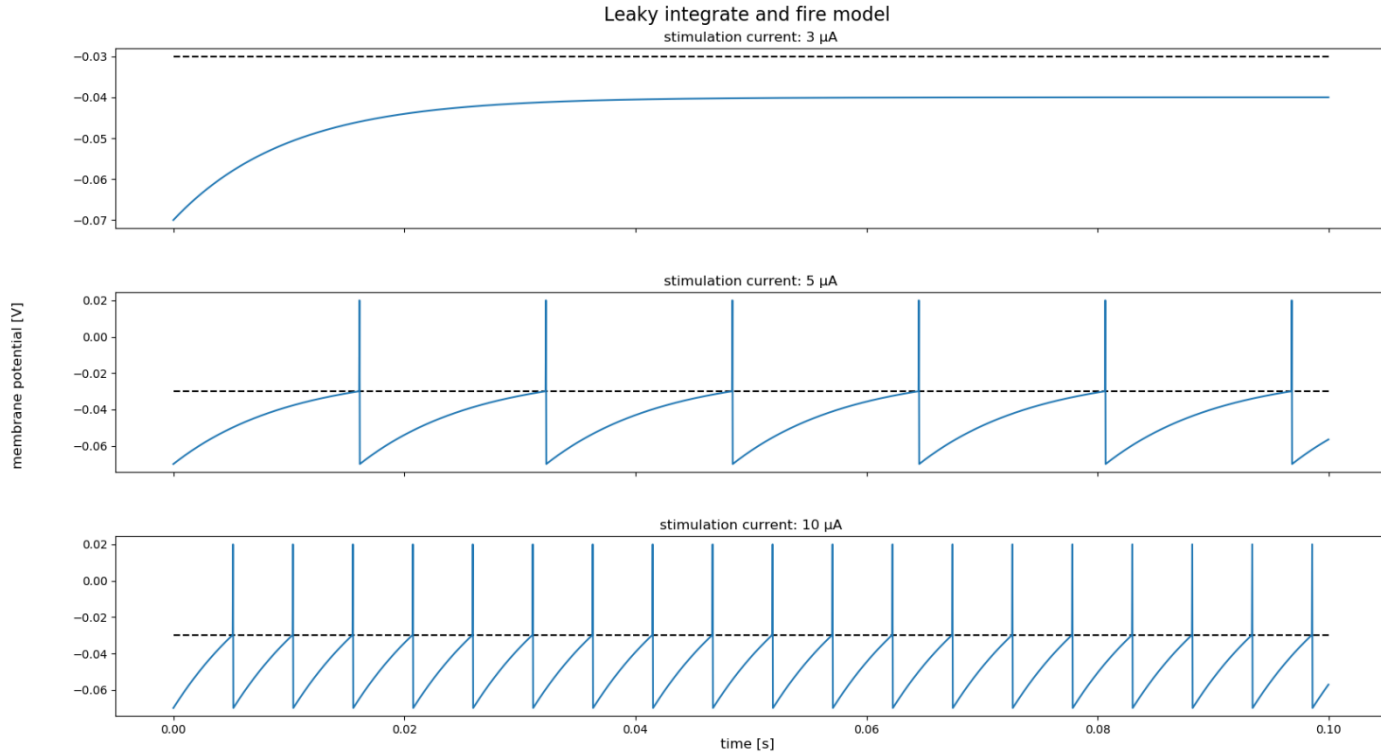


Figure 4: Leaky integrate and fire neuron model. Subplots show data for increasing stimulation current (3, 5, 10 μ A; top to bottom). Dashed lines show the threshold value at -30 mV. The parameters passed to the equation are: $c_m = 1\mu F$, $g_{leak} = 100\mu S$, $V_{rest} = -70$ mV, $V_{Thr} = -30$ mV, $V_{spike} = 20$ mV

In the first case with a stimulation current of 3 μ A the charge of the membrane is not sufficient to exceed the threshold potential (-30 mV). Charge and leakage of the membrane reach a state of equilibrium and thus V_m approaches an asymptotic value. In the other two cases, when the stimulation current is larger than 5 μ A the threshold value is exceeded before a steady state is reached. This results in a rapid overshoot of V_m , an action potential. In a physiological neuron voltage gated ion channels would open, the permeability for cations would change leading to an influx of positive charges into the cell and a rapid increase of membrane potential. Without a refractory phase, which is missing in this model, the “cell” is immediately able to be recharged and to fire again at a constant rate.

The firing rate depends on the level of stimulation current and it is inversely proportional to the membrane capacitance and conductivity. This is because at high capacitance more charge has to be applied to change the membrane potential. At high conductivity, charge carriers are quickly extracted from the cell and the charge is moved in the direction of the resting potential. This also means that the steady state is more likely to occur at lower stimulation levels.

Hodgkin & Huxley Model (HH)

LIF models are relatively easy to understand and provide clear explanations for simple neuronal processes. However, they also quickly reach their limits when simulating more complex behaviour. For more complicated problems, models are used that better describe the intricate biophysical reality of neurons. The first model of this kind was published by Hodgkin and Huxley in 1952. Their work on the giant squid axon enabled the authors to develop a set of equations to describe the biophysical properties of the axon. The equations contain information about the current of the two most important cations: Sodium and potassium. And in addition, a third undetermined leakage current.

As already stated above, the transmembrane current for an ion species can be described with the open probability of the corresponding channels. Hodgkin and Huxley have used a similar formulation for their model. They used the maximum conductivity \hat{g} to describe the transmembrane currents of a particular ion species, this is achieved when all channels for an ion species are opened simultaneously. In this case the opening probabilities can be described as a product of \hat{g} with one or more gating variables. This modulates the effective conductance of these channels between none and maximum conductivity. This idea can also be visualized with an equivalent circuit, in which the channels are implemented by voltage-dependent resistors that selectively regulate the current through the individual channel (

Figure 5).

For this circuit the differential equation for the membrane voltage can be formulated as follows:

$$\frac{dV_m}{dt} = -\frac{1}{C} (I_{Na} + I_K + I_{leak}) \quad (16)$$

$$= -\frac{1}{C} (g_{Na}(V - E_{Na}) + g_K(V - E_K) + g_{leak}(V - E_{leak})) \quad (17)$$

When solved for the steady state condition ($\frac{dV_m}{dt} = 0$) this equation emerges:

$$V_m = \frac{E_{Na} * g_{Na} + E_K * g_K + E_{leak} * g_{leak}}{g_{Na} + g_K + g_{leak}} \quad (18)$$

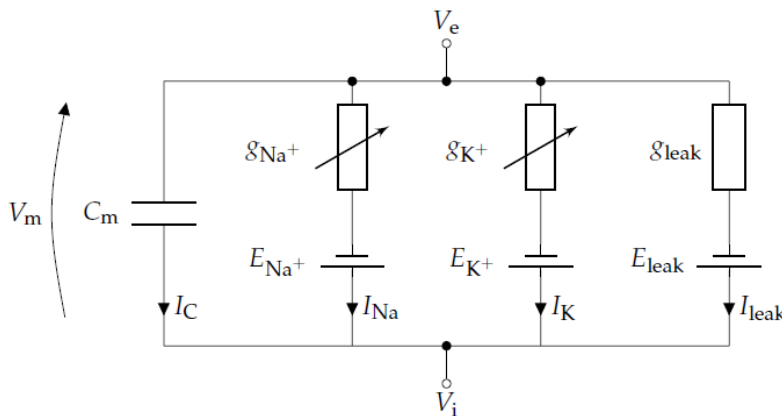


Figure 5: "Equivalent circuit for the Hodgkin Huxley membrane model." Hemmert, W.; Encke J. (2017) p. 22

This equation illustrates the relationship between conductivity, Nernst potential and membrane potential, because the membrane potential is the sum of Nernst potentials for potassium and sodium, which are weighted by their conductivity. Thus, if the conductivity for an ion species increases, the

membrane potential approaches the corresponding Nernst potential. The experimentally determined Nernst potentials for potassium and sodium are $E_{Na} = 115 \text{ mV}$ and $E_K = -12 \text{ mV}$, therefore a change in conductivity modulates the membrane potential between these two values.

In their work Hodgkin and Huxley modelled the opening probability of the potassium channel using the gating variable n^4 . According to the general description for the conductivity g_x of an ion channel:

$$\hat{g}_x = \hat{g}_x \prod_{i=1}^n a_i^{m_i} \quad (19)$$

The following equation is obtained for the potassium channel:

$$K = \hat{g}_K n^4 (V - E_K) \quad (20)$$

Where \hat{g}_K is the maximum conductivity for potassium in $\frac{S}{m^2}$ and E_K is the Nernst potential for potassium in mV. „The power of 4 can be interpreted as a system with 4 independent gating mechanisms each having the open probability n . If all four have to be in open state for the channel to be permeable, we end up with a probability of n^4 “(Hemmert, W., Encke J. (2017), p. 23)

The sodium channel was modelled using two gating variables n and h :

$$Na = \hat{g}_{Na} m^3 h (V - E_{Na}) \quad (21)$$

„The gating variable m^3 describes three activation gates (analogous to n in the sodium channel) while h is a single inactivating gate. For the whole channel to be open, all activating gates as well as the inactivation gate must be open. “(Hemmert, W., Encke J. (2017), p. 23)

The leakage channel behaves like a normal resistance and does not show any gating mechanism.

$$leak = \hat{g}_{leak} (V - E_{leak}) \quad (22)$$

Changes in biological systems rarely occur abruptly, but continuously. Therefore, the differential equation is to be derived, which describes the temporal course of the opening probability for a channel. In the simplest case, such a process is the transition between two states of a system. In this case, the probability of being in one state or another is dependent on voltage-dependent constant rates α and β . The following equation describes this behaviour, the probability that the channel is open is described with P_0 in this case:

$$\frac{dP_0}{dt} = \alpha(V_m)(1 - P_0) - \beta(V_m)P_0 \quad (23)$$

If this equation is applied to the three gating variables of the HH model, the following equations can be returned:

$$\begin{aligned} \frac{dm}{dt} &= \alpha_m(1 - m) - \beta_m m \\ \frac{dn}{dt} &= \alpha_n(1 - n) - \beta_n n \\ \frac{dh}{dt} &= \alpha_h(1 - h) - \beta_h h \end{aligned} \quad (24)$$

Here α_x and β_x are voltage dependent rates between the open and closed state. Hodgkin and Huxley were able to apply their experimental results to these equations to obtain values as a function of the membrane voltage V_m :

$$\begin{aligned}\alpha_m &= \frac{25 \text{ mV} - V_m}{10 \text{ mV} * \left(e^{\frac{10 \text{ mV} - V_m}{10 \text{ mV}}} - 1 \right)} & \beta_m &= 4e^{-V_m/18 \text{ mV}} \\ \alpha_n &= \frac{1 \text{ mV} - 0.1 * V_m}{10 \text{ mV} * \left(e^{\frac{25 \text{ mV} - V_m}{10 \text{ mV}}} - 1 \right)} & \beta_n &= 0.125e^{-V_m/80 \text{ mV}} \\ \alpha_h &= 0.07e^{-V_m/20 \text{ mV}} & \beta_h &= \frac{1}{e^{\frac{30 \text{ mV} - V_m}{10 \text{ mV}}} + 1}\end{aligned}\quad (25)$$

Equations 24 can be understood as exponential growth or decrease to a steady-state state x_∞ , with values between 0 and 1, and a time constant τ_x [sec]. Both values are proportional to the temporal change of the membrane potential.

$$\tau_x(V_m) = \frac{1}{\alpha(V_m) + \beta(V_m)} \quad (26)$$

$$x_\infty(V_m) = \frac{\alpha(V_m)}{\alpha(V_m) + \beta(V_m)} \quad (27)$$

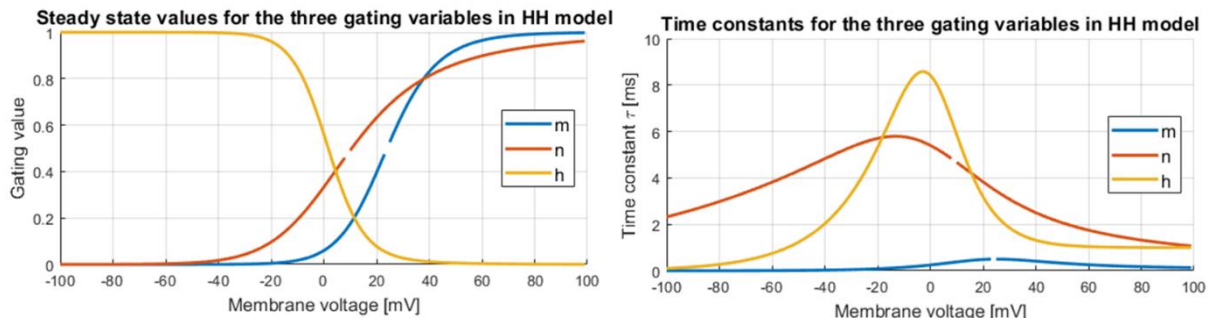


Figure 6: Plot of the steady state values (top) and time constants (bottom) for the three gating variables in HH model

A graphical representation of these values can be found in Figure 6 which corresponds to the original work of H&H, who defined the resting potential as 0 mV. Thus, all values are shifted upwards by about 60 mV. Looking at the steady state values for the rest potential, it is noticeable that the sodium channels (n,h) are almost completely closed, while some potassium channels are open (m). If the membrane is depolarized, both potassium and sodium channels are activated by the m and n gates, but the sodium channels open earlier due to the smaller time constants. The open channels are filled with positively charged cations, which further depolarizes the membrane potential. This feedback loop opens additional sodium channels and V_m approaches the Nernst potential for sodium E_{Na} . In the meantime, the inactivation channel h opens and reduces the influence of sodium. In time the potassium channels react and lead to an outflow of positive charge carriers (K^+). When the K^+ outflow exceeds the influence of Na^+ , the membrane potential begins to decrease again and both channels close due to the influence of n and m. During the refractory phase, the time constant τ_m comes into play, it is smaller than the other constants and causes the sodium channels to close relatively quickly. Sodium and potassium channels close with a time delay, which leads to a temporary hyperpolarization with values below the resting potential. This reaction can also be seen in Figure 7.

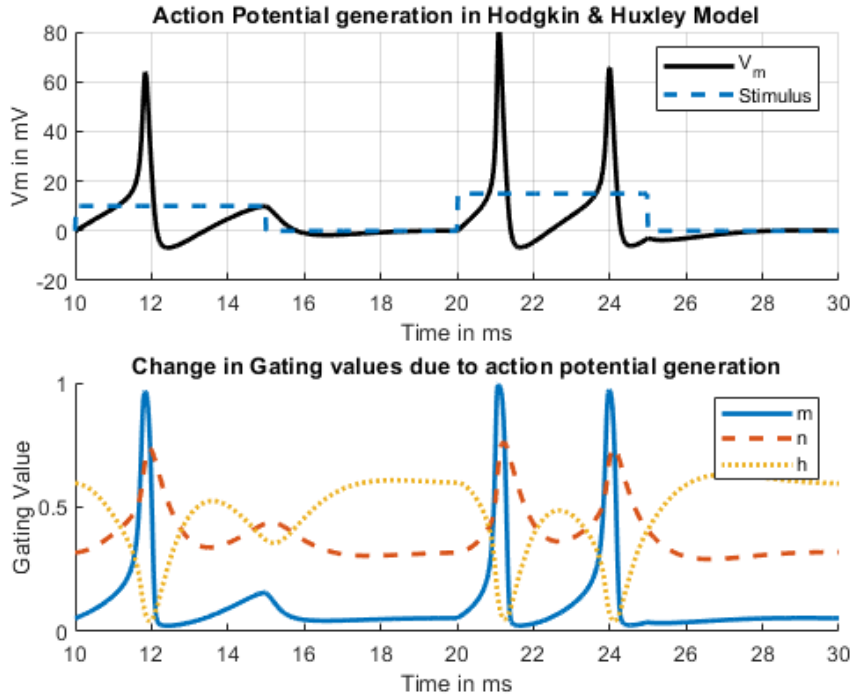


Figure 7: Top plot: Change of Membrane potential in reaction to stimulation current: $I_{stim}(10 - 15 \text{ ms}) = 10 \mu\text{A}$, $I_{stim}(20 - 25 \text{ ms}) = 15 \mu\text{A}$. Bottom plot: Change in Gating values due to stimulation. Time frame shared among plots. Temperature = 25°C , $c_m = 1 \mu\text{F/cm}$, sampling frequency = 44200 Hz

Hodgkin and Huxley conducted their experiments at 6.3°C , a value far below the normal body core temperature of animals. Since the underlying processes follow the Boltzmann statistics, an increase in temperature has a positive influence on the reaction rate. In order to compensate for these temperature differences, a compensation factor k was introduced into the gating equation:

$$\frac{dx}{dt} = k\alpha_x(1 - x) - k\beta_x x \quad (28)$$

The compensation factor was calculated as following:

$$k = Q_{10}^{T-T_0/10^\circ\text{C}} \quad (29)$$

“Where the Q_{10} value is often chosen around 3 so that a temperature increase of 10°C results in three times lower time constants T_0 is the Temperature at which the data was collected (for the HH model $T_0 = 6.3^\circ\text{C}$).” Hemmert, W.; Encke J. (2017) p.25

Another interesting parameter of the model is the rheobase current, i.e. the current that has to be applied in order to exceed the threshold potential:

$$I_{stim} = \frac{V_{th} - V_{rest}}{R_m(1 - e^{-T_{stim}/\tau})} \quad (30)$$

This formula can be simplified for the case that the exact rheobase current is applied the time to spike will be infinitive. With this knowledge the rheobase current can be calculated using:

$$T_{stim} \gg \tau \quad I_{stim} \approx \frac{V_{thr} - V_{rest}}{R_m} \quad (31)$$

Since in the HH model conductivities are considered, these values must be converted into resistance in order to be able to insert them into the formula. It applies $R = \frac{1}{g}$ with the values $g_{Na} = 120 \frac{\text{mS}}{\text{cm}^2}$,

$g_K = 36 \frac{\text{mS}}{\text{cm}^2}$, $g_{leak} = 0.3 \frac{\text{mS}}{\text{cm}^2}$. And a parallel connection is present, therefore the following applies:

$$g_{ges} = \sum_{n=1}^N g_n \quad (32)$$

$$\frac{1}{R_{ges}} = \sum_{n=1}^N \frac{1}{R_n} \quad (33)$$

A resistance of $R_{ges} = 6.398 \frac{m\Omega}{cm^2}$ is calculated. With the values for $V_{thr} = -30 mV$ and $V_{rest} = -70 mV$ a rheobase current of 6.25 A results. This value seems too high, the literature (Hemmert, W.; Encke J. (2017) p. 25) speaks of currents in the nA range and stimulation with 10 μA current did elicit AP in Figure 7. One reason for this is certainly the unit of conductivity in mS/cm^2 . It is unclear to me how this can be converted into an area-independent unit.

This formula shows that $I_{Rheobase}$ only depends on the membrane resistance and not on the capacity. This can be explained by the RC behaviour of the membrane. "With a long pulse duration, the capacitance behaves like an insulator leaving only the resistance. While on the other hand, for very short pulses (if $T \ll \tau$) we can simplify Eq. 30 by approximating $1 - e^{-T/\tau}$ so that we gain:" (Hemmert, W.; Encke J. (2017) p. 21)

$$T_{stim} \ll \tau \quad I_{stim} \approx \frac{C_m(V_{thr} - V_{rest})}{T_{stim}} \quad (34)$$

In this case, the term only depends on the capacity. The total charge that must be induced to trigger an action potential (*threshold charge* Q_{thr}) in this case is $I_{stim} * T_{stim}$. This leads to the conclusion that Q_{thr} is constant for short pulses (Eq. 35) while increasing with T_{stim} for long pulses (Eq. 36).

$$T_{stim} \ll \tau \quad Q_{thr} \approx C_m(V_{thr} - V_{rest}) \quad (35)$$

$$T_{stim} \gg \tau \quad I_{stim} \approx T_{stim}(V_{thr} - V_{rest})/R_m \quad (36)$$

Passive Cable neuron model

The previous models treated the neuron as a homogeneous electrical unit. In reality however, the cell consists of different areas, the soma, axons and dendrites, which can be heavily branched in themselves. In addition, there are different ion channel densities along the same cell. In the following we will describe a model that incorporates the morphological characteristics of a neuron.

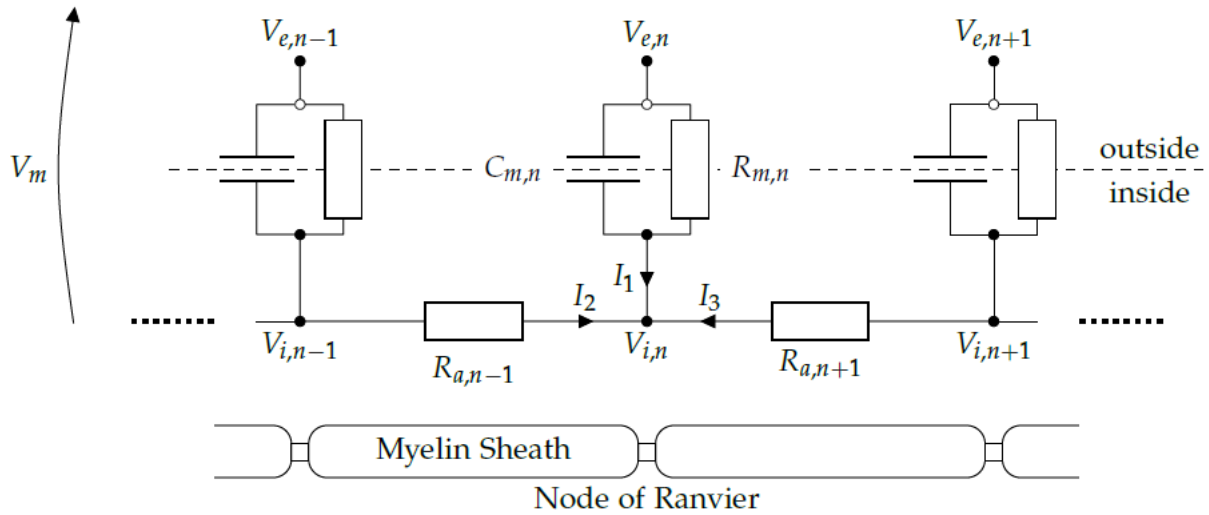


Figure 8: "Equivalent circuit for a short piece of axon. Each node of Ranvier is modeled as a RC element while the myelin sheath is modeled as a simple resistance." Source: Hemmert, W.; Encke J. (2017) p. 26

Myelination is an important part of the morphology. Myelinated axons consist of a fixed sequence of Ranvier nodes and myelin sheaths. Each node can be considered as a self-contained unit and the membrane of each unit can be modelled as an RC element and the compartments are connected via myelin sheaths. Since no voltage drops across the myelin-isolated membrane, this can be interpreted as a simple resistor. The replacement circuit for this model can be found in Figure 8.

For the derivation of the equations in this model we use Kirchhoff's first law (Eq. 2) for the central node of each compartment.

$$0 = I_1 + I_2 + I_3 \quad (37)$$

In this case, I_1 is the current across the diaphragm and can also be written as:

$$I_1 = \frac{V_{i,n} - V_{e,n}}{R_{m,n}} + C_{m,n} \frac{\delta(V_{i,n} - V_{e,n})}{\delta t} \quad (38)$$

„Where $V_{i,n}$ is the potential on the inside and $V_{e,n}$ the potential on the outside of the nth compartment while $R_{m,n}$ and $C_{m,n}$ are the compartment's membrane resistance and capacitance. For the following section, we will assume these to be constant for all compartments." Hemmert, W.; Encke J. (2017) p.27

The currents I_2 and I_3 of the adjacent compartments are described with the following equations:

$$I_2 = \frac{V_{i,n} - V_{i,n-1}}{R_{a,n-1}} \quad (39)$$

$$I_3 = \frac{V_{i,n} - V_{i,n+1}}{R_{a,n+1}} \quad (40)$$

$R_{a,n-1}$ and $R_{a,n+1}$ are axonal resistances of the preceding and following compartments respectively (see Figure 8). It is assumed that these resistances are constant for all compartments. "If we now substitute $V_i - V_e$ in eq. 38 with the membrane potential V_m , we gain the differential equation: " Hemmert, W.; Encke J. (2017) p.27

$$0 = \frac{V_{m,n}}{R_m} + C_m \frac{\delta V_{m,n}}{\delta t} - \frac{V_{i,n-1} - 2V_{i,n} + V_{i,n+1}}{R_a} \quad (41)$$

„This equation depends on the unknown internal potential V_i which can be replaced with $V_m + V_e$.“
Hemmert, W.; Encke J. (2017) p.27

$$C_m \frac{\delta V_{m,n}}{\delta t} = -\frac{V_{m,n}}{R_m} + \frac{V_{m,n-1} - 2V_{m,n} + V_{m,n+1}}{R_a} + \frac{V_{e,n-1} - 2V_{e,n} + V_{e,n+1}}{R_a} \quad (42)$$

As a further simplification, we assume that the external potential along the compartments is constant ($V_{e,n} = V_{e,n+1} = V_{e,n-1}$). Thus, the differential equation for the passive cable neuron looks like this:

$$\frac{\delta V_{m,n}}{\delta t} = \frac{1}{C_m} \left(\underbrace{-\frac{V_{m,n}}{R_m}}_A + \underbrace{\frac{V_{m,n-1} - 2V_{m,n} + V_{m,n+1}}{R_a}}_B \right) \quad (43)$$

As in the previous models, a change in the membrane potential V_m leads to a charge/discharge of the membrane capacity C_m . The capacity can be charged by two different currents, which are labelled A and B in the equation above. The term A contains all non capacitive currents through the membrane, i.e. all currents passing through the membrane resistor. Term B contains all currents which originate from neighbouring compartments or are discharged to them.

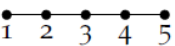
Morphology	Connection Matrix
	$\begin{pmatrix} -1 & 1 & 0 & 0 & 0 \\ 1 & -2 & 1 & 0 & 0 \\ 0 & 1 & -2 & 1 & 0 \\ 0 & 0 & 1 & -2 & 1 \\ 0 & 0 & 0 & 1 & -1 \end{pmatrix}$

Figure 9: Simple linear neuron morphology and its corresponding connection matrix. Hemmert, W.; Encke J. (2017) p.28

The equation can be represented as a matrix in Matlab for the purpose of graphical representation and implication. For this purpose, a vector V_m is introduced. The final matrix form is also called connection matrix and reflects the morphology of the neuron. The negative values on the diagonal of each row can be understood as the number of connected compartments. The ones in the columns indicate which compartments are connected to each other. E.g. compartment 3 is connected to comp. 2 and 4. Theoretically complex branching patterns are possible, but in the following only the simple case of a linear morphology is considered (Figure 9).

For the transition from the discrete, myelinated to the continuous, unmyelinated view of the axon, the following parameters are converted into length independent forms: C_m , R_m and R_a to c_m , r_m and r_a utilizing the following equations:

$$R_m = \frac{\rho_m d_m}{2\pi a * \Delta l} = \frac{r_m}{\Delta l} \quad (44)$$

$$C_m = \frac{\epsilon_r \epsilon_0 2\pi a * \Delta l}{d_m} = c_m * \Delta l \quad (45)$$

$$R_a = \frac{\rho_a * \Delta l}{\pi a^2} = r_a * \Delta l \quad (46)$$

Here a is the radius of the neuron, Δl is the length of a compartment in meters and d_m is the thick

ness of the membrane. ρ_m and ρ_a are specific resistances of the membrane and the axon in Ωm , ε_0 is the electrical field constant and ε_r is the electrical conductivity of the membrane.

$$\frac{\delta V_{m,n}}{\delta t} = \frac{1}{c_m} \left(-\frac{V_{m,n}}{r_m} + \frac{1}{r_a} \frac{V_{m,n-1} - 2V_{m,n} + V_{m,n+1}}{\Delta l^2} \right) \quad (47)$$

Assuming Δl converges to 0, the finite difference then converges to a differential equation, given by:

$$c_m \frac{\delta V_m}{\delta t} = -\frac{V_m}{r_m} + \frac{1}{r_a} \frac{\delta^2 V_m}{\delta x^2} \quad (48)$$

$$r_m c_m \frac{\delta V_m}{\delta t} = -V_m + \frac{r_m}{r_a} \frac{\delta^2 V_m}{\delta x^2} \quad (49)$$

This equation is also known as the cable equation. This partial differential equation can be solved for the steady state ($\frac{\delta V_m}{\delta t} = 0$). This results in:

$$V(x) = V_0 e^{\frac{-x}{\lambda}} \quad (50)$$

$$\lambda = \sqrt{\frac{r_m}{r_a}} \quad (51)$$

Here V_0 is the potential at point $x = 0$. In other words: If a potential of V_0 is applied to the axon at point $x = 0$, the potential drops exponentially, along the axon length. The distance that a graded electric potential will travel along a neuron via passive electrical conduction is given by λ . As in the previous Hodgkin and Huxley model the time constant τ can be calculated as the product of its resistance and capacity:

$$\tau_m = r_m c_m \quad (52)$$

These values can be inserted into the cable equation to derive the final form of the cable equation:

$$\tau \frac{\delta V_m}{\delta t} + V_m = \lambda^2 \frac{\delta^2 V_m}{\delta x^2} \quad (53)$$

This formula was implemented in MATLAB to create the plots shown in Figure 10.

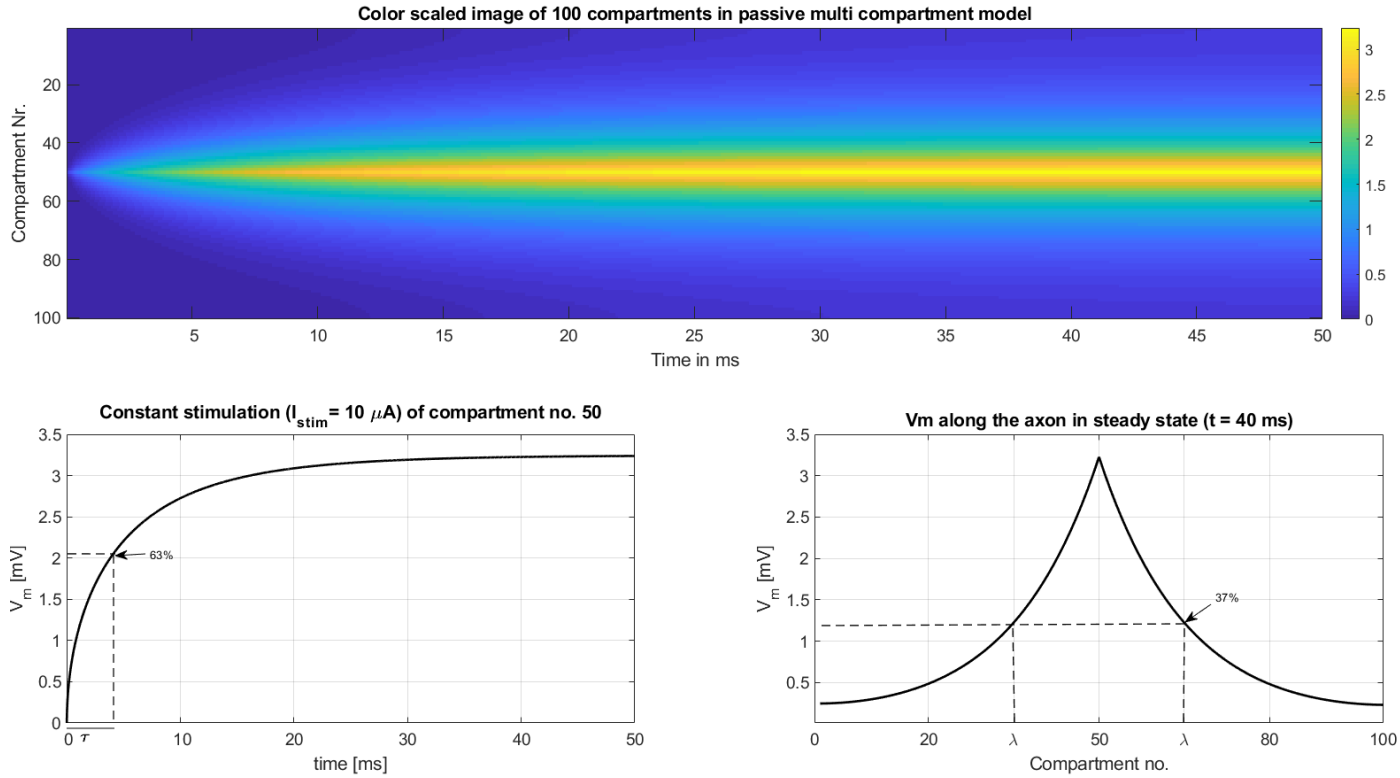


Figure 10: The Passive Unmyelinated Axon Model (linear morphology). Top: Constant excitation ($10 \mu A$) in compartment 50 and spread of excitation along the axon to neighbouring compartments in a colour scaled image. Bottom left: Asymptotic rise of the membrane potential in the stimulated compartment. τ is the time constant. Bottom right: Asymptotic decay of V_m along the axon in steady state ($t = 20$ ms). λ is the length constant. Parameters used: $V_{rest} = -70$ mV, $C_m = 1 \mu F/cm^2$, $\rho_{axon} = 0.1 k\Omega cm$, $r_{axon} = 2 * 10^{-4} cm$, $l_{comp} = 0.3 * 10^{-4} cm$

The upper plot shows the membrane voltage for 100 compartments connected in series (see Figure 9) over a time frame of 50 ms. Compartment 50 is stimulated at a constant level of $10 \mu A$, leading to an asymptotic increase of V_m until it reaches the steady state of ~ 3.3 mV after ~ 20 ms (Figure 10 bottom left). The current spreads from the site of excitation to neighbouring compartments along the axon, raising their Membrane voltage until the current is dissipated by leakage out across the axon membrane (Figure 10 bottom right).

The time- and length constant in this case was calculated by the simple ratio of $1 - 1/e$ of the membrane voltage maximum value and plotted in Figure 10. For the exact calculation of these values, the thickness of the axon d_m in equations 44 and 45 is missing.

The rough estimate for the time constant is: $\tau \approx 4.1$ ms (2.05 mV), the estimate for the length constant is: 15 compartments and/ or $\lambda = 4.5 * 10^{-4} cm$.

Active Axon Model

In order to move from the passive model to an active one that can trigger action potentials, in the next step ion channels are added to the eq. 43. For this purpose, the part of the equation described as A, i.e. all non-capacitive currents, is replaced with the Hodgkin and Huxley currents from above:

$$\frac{\delta V_{m,n}}{\delta t} = \frac{1}{C_m} \left(-I_{m,n} + \frac{V_{m,n-1} + 2V_{m,n} + V_{m,n+1}}{R_a} \right) \quad (54)$$

$$I_{m,n} = I_{Na,n} + I_{K,n} + I_{leak,n} \quad (55)$$

The value $I_{m,n}$ must be recalculated for each compartment because the membrane potential also differs between two adjacent compartments. Due to the newly introduced ion channels, each compartment is now able to fire AP. If such a burst is triggered it spreads along the axon and triggers further AP, propagating the signal. Figure 11 top left shows two initial action potentials triggered by stimulating compartments 33 and 66. The AP propagates along the axon (Figure 11 top right) in both directions, resulting in four action potentials running simultaneously on the same axon (Figure 11 bottom left). In the event of two action potentials meeting (~ 16 ms), there is no redirection because both compartments involved are within their absolute refractory period and are therefore unable to be excited again. The velocity at which the signal propagates can be seen in Figure 11 top right, where the membrane voltage of four adjoining compartments are shown.

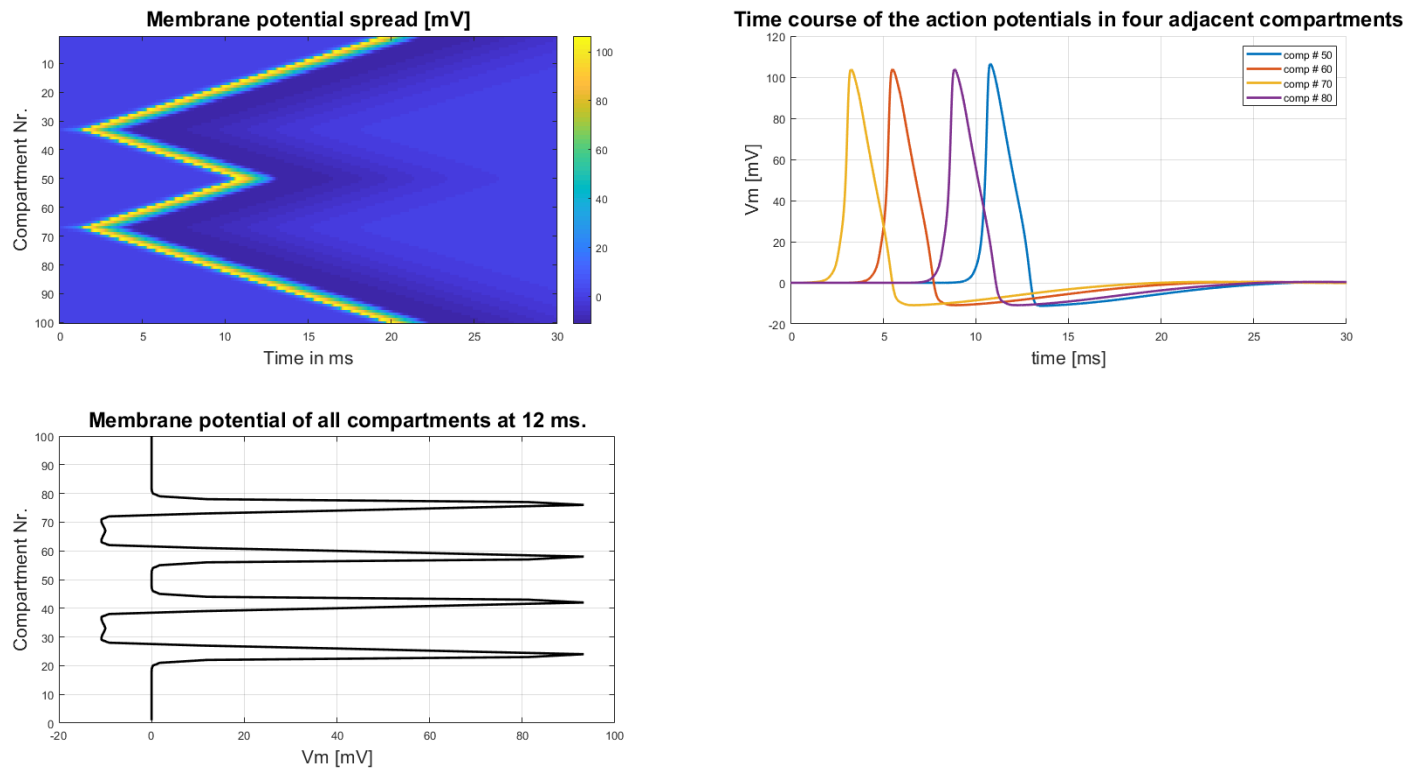


Figure 11: Top left: Spread of excitation from two sources in an active multi compartment model, Top right: Time course of action potential being generated in four adjacent compartments (#50 to #80) Bottom left: Membrane Voltage of all compartments in a given time frame (12 ms).

The Activating Function - External Stimulation of Neurons

In the previous consideration it was assumed that the extracellular potential $V_{e,n}$ is constant over all nodes in order to be able to eliminate the V_e dependent part of the cable equation. In order to find out how a neuron reacts to stimulation by external electrodes, this part must be reintroduced:

$$\frac{\delta V_{m,n}}{\delta t} = -\frac{1}{C_m} I_{HH,n} + \frac{1}{C_m} \frac{V_{m,n-1} + 2V_{m,n} + V_{m,n+1}}{R_a} + \underbrace{\frac{1}{C_m} \frac{V_{e,n-1} + 2V_{e,n} + V_{e,n+1}}{R_a}}_{\text{Activating Function}} \quad (56)$$

As this term describes the activation of the neuron due to an external potential, it is also called the activating function. If one assumes, as with the passive description of the neuron, that the length of a compartment converges to 0, one concludes that the activation function converges to a second order differential equation:

$$\lim_{\Delta l \rightarrow 0} \frac{1}{C_m} \frac{V_{e,n-1} + 2V_{e,n} + V_{e,n+1}}{R_a} = \frac{1}{C_m r_a} \frac{\delta^2 V_e}{\delta x^2} \quad (57)$$

An interpretation of this equation is, that a neuron is stimulated by the second derivative of the external potential along the axon. This means that if the same external potential is applied to all compartments, there will be no change in the membrane potential. This is because the extracellular and intracellular potential are in a state of flow equilibrium. If, on the other hand, the external voltage is applied to only one compartment, a local difference in intracellular potential occurs, resulting in currents from adjacent areas to compensate for the difference (Figure 12).

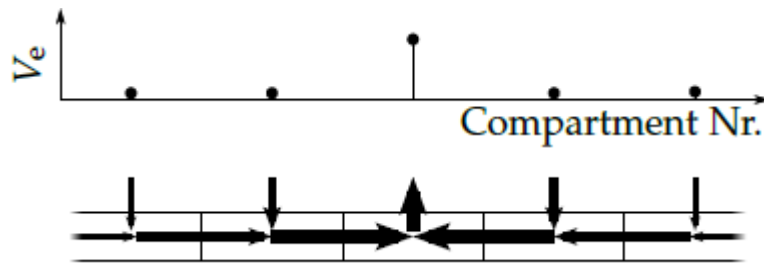


Figure 12: “Increasing the external potential at the central compartment (plotted at the top) also raises the internal potential in the same compartment which leads to equalizing currents from the neighbouring compartments which has to be counteracted by discharging the membrane capacity.” Source: Hemmert, W.; Encke J. (2017) p.32

These currents I_2 and I_3 have the same properties as the currents of the passive axon model described above (Figure 8). The net influence in the central compartment must be compensated by discharging the membrane capacity, this reduces the membrane potential. In case a constant electric field is applied to the axon, there would be a constant change in potential at each point. This would cause two identical currents with opposing signs to flow into each compartment, without changing the membrane potential. If the two above-mentioned points are taken together, the conclusion can be drawn that a neuron is only effectively stimulated when there is a change in the slope with which the external potential changes.

Stimulation with a point current source

The simplest form of electrical stimulation with an external electrode consists of a point current supply in a homogeneous medium and an earth electrode infinitely far away from the point of stimulation. “In this case, the electrical potential φ (in volt) at a distance r (in meter) from the electrode can be calculated as:

$$\varphi = \frac{\rho}{4\pi} \frac{I_{stim}}{r} \quad (58)$$

Where ρ is the specific electrical resistance of the medium in Ωm and I_{stim} the stimulation current in ampere. “ Hemmert, W.; Encke J. (2017) p.33f

$$f_{activating} = \frac{1}{c_m r_a} \frac{\delta^2 V_e}{\delta x^2}$$

$$= \frac{\rho}{4c_m r_a \pi} \frac{I_{stim}(d - 2x^2)}{(d + x^2)^{5/2}} \quad (59)$$

Developing a cochlea implant algorithm

With this theoretical knowledge and the developed neuron models a continuous interleaved sampling (CIS) algorithm was to be written, which imitates the acoustic process performance of a cochlear implant. This strategy encodes speech features implicitly by accurately representing the spectro-temporal structure of the speech signal. The basic idea of this is to divide the incoming sound into a number of frequency bands. Extracting the temporal envelope in each band and using a compressed version of the envelope to modulate a fixed rate-train of pulses on each electrode. These pulse trains are eventually sent to each electrode interleaved in time to prevent unwanted interactions. CIS involves four stages of signal processing (Figure 13).

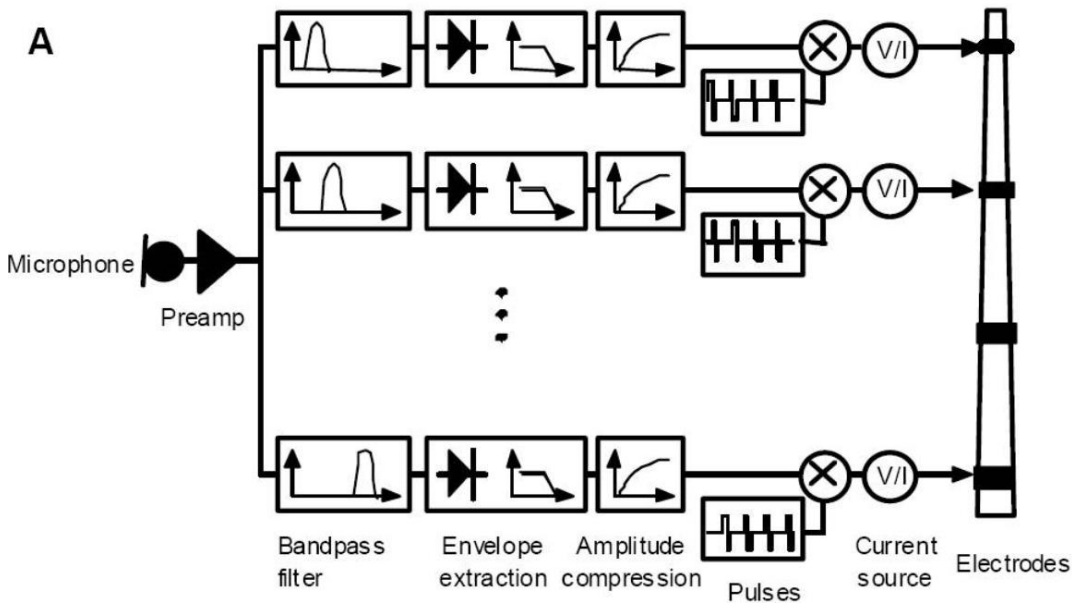


Figure 13: A. Block diagram and signal processing in the Continuous-Interleaved-Sampling (CIS) strategy. Source: Zeng et al. 2008

CIS Step 1 – Bandpass filters

Bandpass filters are used to map the acoustic broadband signal with a limited number of electrodes. In the following example, frequencies below 500 Hz and above 4000 Hz were attenuated in a first step. Subsequently, a filter bank with 10 bandpass filters (matches the number of electrodes) evenly spaced between 500 and 4000 Hz was used. Since for practical reasons the electrode array cannot be inserted all the way to the apex of the cochlea, the choice of this filter offers a good compromise between the frequency presentation and the unnatural frequency to place mapping (Figure 14). This means that the natural greenwood frequency of the hair cell to their corresponding auditory neurons is no longer given. This is not a big problem as the functional connection between the hair cell and the auditory nerve is damaged anyway.

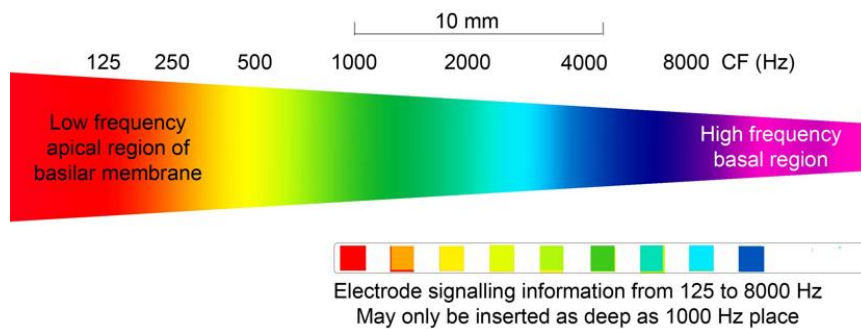


Figure 14: compromise between the frequency presentation and the unnatural frequency to place mapping visualized. Ref: „neuropro auditory 4.pptx “lecture slides

CIS Step 2: Envelope extraction

In CIS, only the envelope of the acoustic signal i.e. modulation of the amplitude is transmitted. This preserves the temporal structure of the signal, which can be used to detect vowels in low frequency ranges. The temporal coding is the result of the functional polarization of the hair cells. which means that deflection of the stereocilia in one direction is excitatory for the hair cells and movement in the opposite direction is inhibitory. The result is a train of nerve impulses time locked to the individual cycles of the acoustic stimulus. Due to the refractory phase, a single hair cell cannot respond to every cycle of a signal, especially at higher frequencies. A population of nerve fibers all phase-locking to the same stimulus, represent in their combined discharge pattern the complete temporal representation of the stimulus

For this purpose, a low-pass filter with a cut-off frequency of 200 Hz and full wave rectification was used.

CIS Step 3: Compression & conversion to current level

The envelope outputs were then compressed. This is necessary because with electrically evoked hearing the dynamic range is much smaller (6 - 26 dB) than with acoustic hearing (Pfungst and Xu 2004). The dynamic range in this case is the difference between the threshold value (T) and a current at which the maximum comfortable volume is reached (C). The loss of cochlear compression (caused by the outer hair cell function) produces much steeper rate-intensity functions in electric stimulation than in acoustic stimulation (Javel and Shepherd, 2000). To adapt the stimulus from Pascal to μA it was multiplied by a factor of 700.

CIS step 4: generation of modulated pulse trains

“To avoid electrode interactions caused by electrical field overlap in simultaneous stimulation, which conceivably can smear the band-specific envelope cues, the envelope from each subband is then amplitude-modulated to a high-rate (>800 Hz) pulsatile carrier that interleaves with pulsatile carriers from other subbands. In other words, only one electrode is being stimulated at any given time. “ (Zeng 2004)

The four CIS steps are visualized in Figure 15.

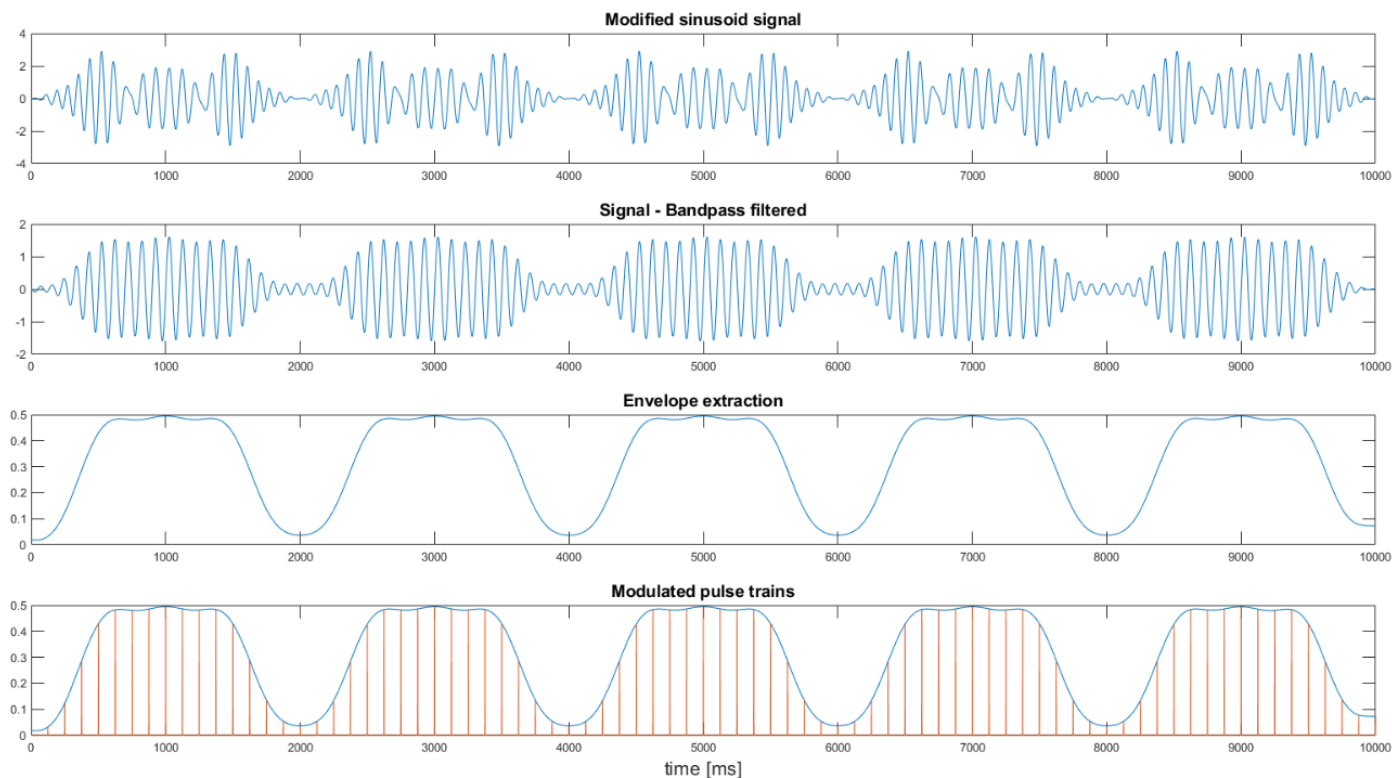


Figure 15: Visualization of CIS steps. From top to bottom: 1 - Bandpass filtered [500 4000] Hz self-generated audio signal. 2 - 10 evenly distributed bandpass filters between 500 and 4000 Hz were. Here and in the following plots channel 4 is shown as an example. 3 - Envelope of the signal. 4 - Modulated pulse trains with a frequency of 800 Hz fitted to the envelope.

Using the models developed above, it is now possible to simulate the response of a single neuron, as well as an accumulation of many neurons, to CIS stimulation. Figure 16 shows the response of a cell to the stimulation of channel 4. It shows a rapid sequence of spikes starting from a stimulation of $>250 \mu\text{A}$ with an increase of the membrane potential of more than 70 mV. Between the spikes and during stimulation with low current there are smaller increases of V_m without triggering spikes. The bottom plot shows pulse trains of successive channels interleaved in time and it also demonstrates the charge balance.

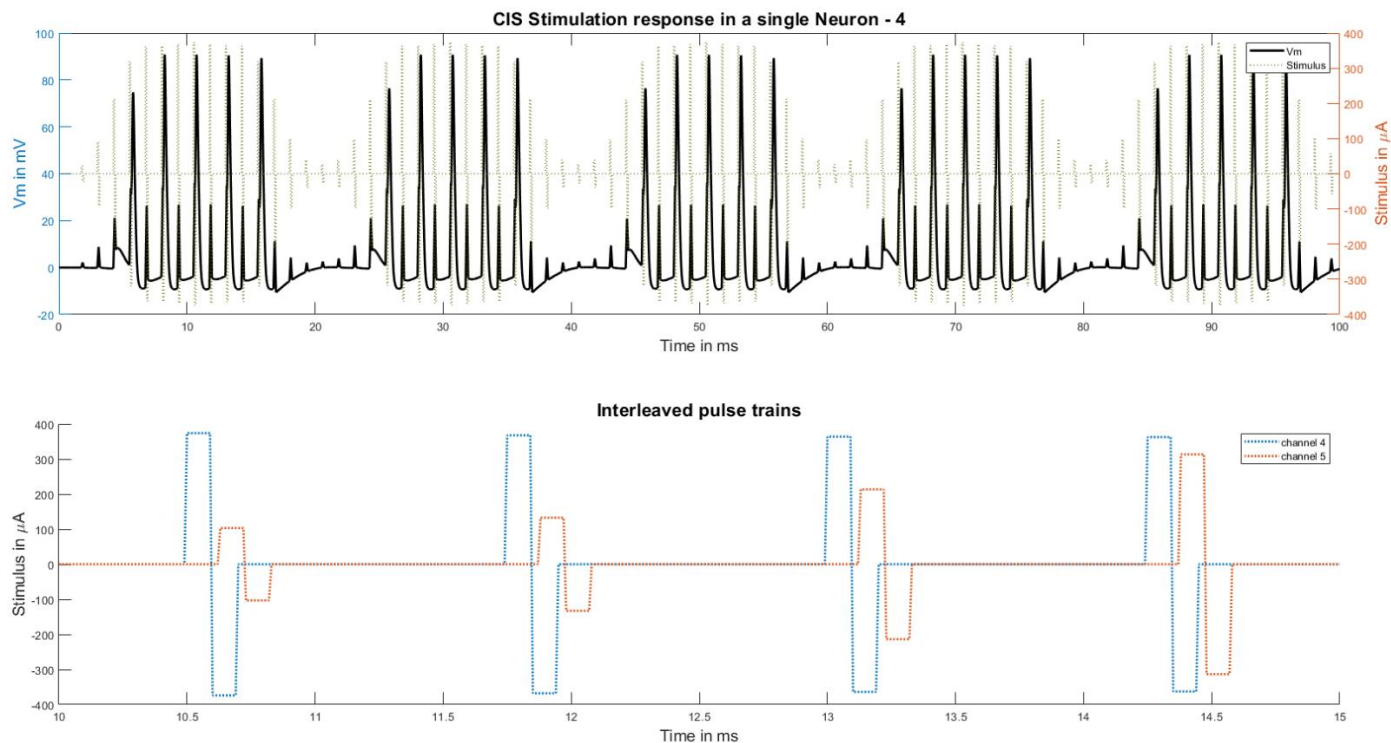


Figure 16: Top: Change in Membrane voltage due to CIS stimulation of channel 4 according to the Hodgkin-Huxley model in a single neuron. Notice the different y axis for Vm and Stimulus. Bottom: 5 ms time frame from above and only Stimulus axis to show interleaved pulse trains.

The multi compartment model is shown in Figure 18. 100 cells were calculated, for which a weighting matrix was applied. This matrix weights 21 cells each with a value between 0 and 1. The peak values are evenly distributed between cells 11 and 90. Thus, it is possible to simulate the stimulation of the 10 electrode channels on 100 cells. The first cells are excited by the lowest frequencies, the last ones by the highest and in between the excitation is evenly distributed.

The stimulation in this model mainly excites the neurons 35 to 50 which corresponds to a frequency range of 1600 to 2200 Hz (see Figure 17). For a given point in time only a handful of cells are active at the same time, the temporal course of Figure 15 can also be seen again. Areas with only low stimulation do not lead to the triggering of action potentials. This pattern of stimulation is transmitted to the spiral ganglia through the cochlea implant, allowing the CI-wearing person to perceive an acoustic representation of the environment. In this case, the signal is very simple and consists only of sinus waves, but a more complex signal can be transmitted with the same underlying algorithm. Today's commercial CI manufacturers use this CIS algorithm.

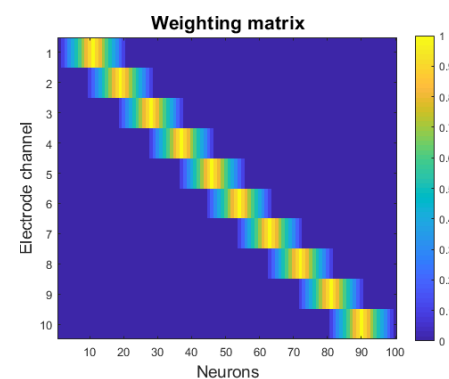


Figure 17: Weighting matrix for multi compartment model

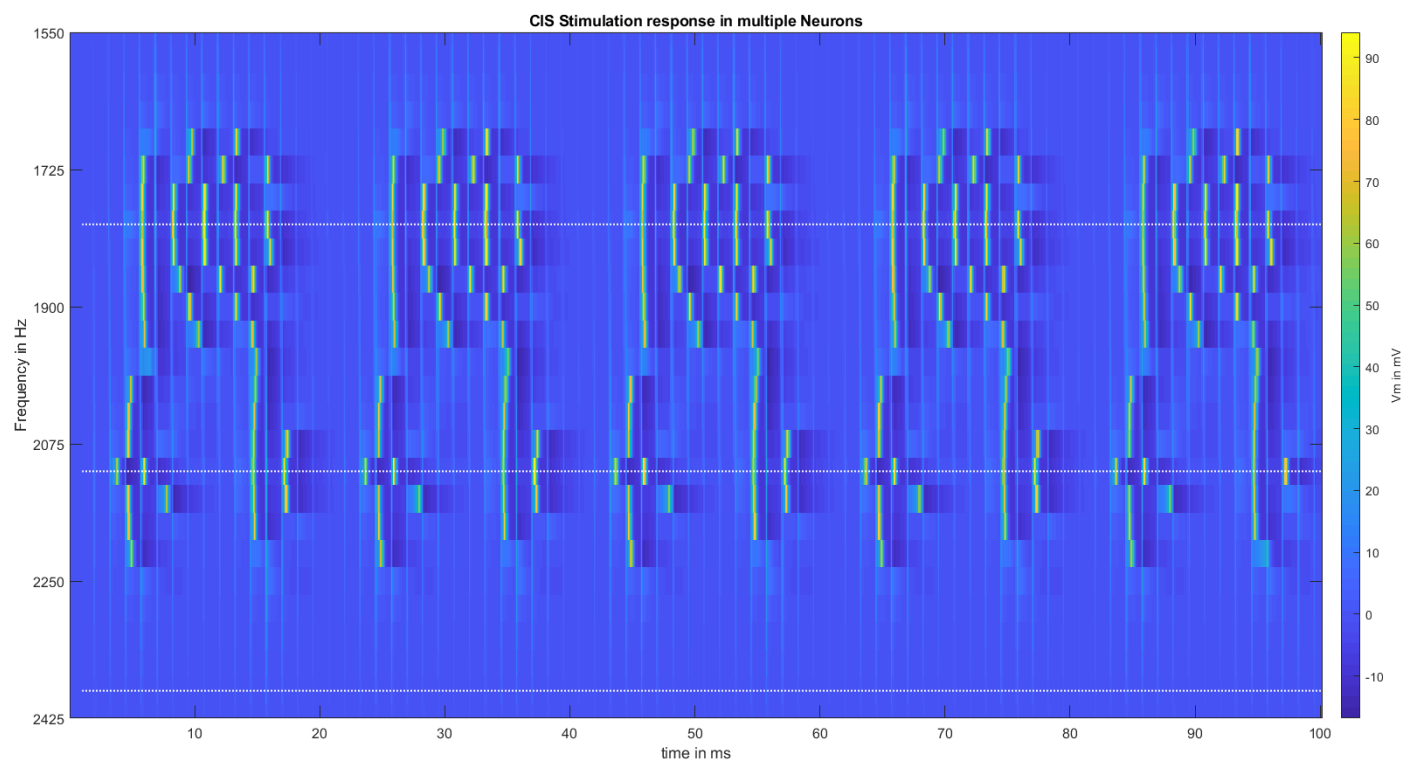


Figure 18: Change in Membrane voltage due to CIS stimulation in a multi compartment according to the Hodgkin-Huxley model

Publication bibliography

Pfingst, Bryan E.; Xu, Li (2004): Across-site variation in detection thresholds and maximum comfortable loudness levels for cochlear implants. In *Journal of the Association for Research in Otolaryngology* : JARO 5 (1), pp. 11–24. DOI: 10.1007/s10162-003-3051-0.

Purves, Dale; Augustine, George J.; Fitzpatrick, David; Hall, William C.; LaMantia, Anthony-Samuel; Whie, Leonard E. et al. (Eds.) (2012): *Neuroscience*. 5th edition. Sunderland, Massachusetts, U.S.A.: Sinauer Associates Inc.

Zeng, Fan-Gang (2004): Trends in cochlear implants. In *Trends in amplification* 8 (1), pp. 1–34. DOI: 10.1177/108471380400800102.

Hodgkin, A. L.; Huxley, A. F. (1952): A quantitative description of membrane current and its application to conduction and excitation in nerve. In *The Journal of Physiology* 117 (4), pp. 500–544.

Hemmert, W.; Encke J. (2017): *Neuroprothetics*, TU-München: Electrical Engineering, version: 0.5.1

Zeng FG, Rebscher S, Harrison W, Sun X, Feng H. Cochlear implants: system design, integration, and evaluation. *IEEE Rev Biomed Eng*. 2008; 1:115–142. doi:10.1109/RBME.2008.2008250